Perturbative approach for surface plasmon effects on flat interfaces periodically corrugated by subwavelength apertures

P. Lalanne, C. Sauvan, J. P. Hugonin, J. C. Rodier, and P. Chavel

Laboratoire Charles Fabry de l'Institut d'Optique, Centre National de la Recherche Scientifique, Université Paris XI,
BP 147, F-91403 Orsay Cedex, France

A perturbative approach for surface-plasmon-related effects encountered in metallo dielectric interfaces that incorporate periodic subwavelength defects with arbitrary shapes or materials is presented. It provides a simple insight into the physics of some important optical properties of these interfaces. We apply this understanding to one and two-dimensional metallic membranes perforated by subwavelength apertures and other related gratings geometries. The approach accounts quantitatively for the nearly null transmission of these membranes in the surface plasmon frequency band. It also predicts phenomena like an antisymmetric surface plasmon resonance for gratings with a vertical mirror symmetry at very small incidences and the possible absence of any reflection when outcoupling from an array of subwavelength slits into free space.

I. INTRODUCTION

For more than a century, the optical response of metallic gratings has constituted a topic of many experimental and theoretical investigation.[1,2] This response encompasses a rich variety of phenomena, which manifest themselves as rapid variations in the intensity of the various diffracted orders in certain narrow frequency bands. These phenomena are often unexpected and even counterintuitive. For instance, a sinusoidal metallic grating with a modulation depth as small as $\lambda/20$ may totally absorb the incident illumination for some specific frequencies and angles of incidence.[3] These phenomena are called Wood's anomalies and are well understood nowadays from both surface plasmon (SP) physics[1] and more quantitative mathematical models.[2] They are due to the resonant excitation of leaky waves (SP waves) supportable by the grating. The leaky wave possesses a complex parallel wave vector which reflects the fact that, as it propagates, it radiates into one or more radiating space harmonics. Most of the work performed on these anomalies are related to reflection grating with continuous profiles.[1,2] With the recent advances in nanotechnology, there has been a renewed interest in exploiting the optical response of metallic materials periodically corrugated by subwavelength defects. Examples are the trapping of light in small volumes,[4] the anomalous transmission of light through metallic gratings with subwavelength holes,[5] and waveguiding with lateral mode sizes well below the diffraction limit.[6,7]

The objective of this work is to propose a perturbative theory for SP-related effects encountered in metallodielectric interfaces that incorporate periodic subwavelength defects with arbitrary shape or material. The perturbative approach relies on simple forms for the electromagnetic field which are periodically null and strictly satisfy Maxwell's equations on a flat metallic interface and which are expected to remain approximately valid if an array of subwavelength defects are incorporated at the periodically null-field locations. The approach cannot model all SP effects of such engineered interfaces, especially effects related to localized SPs. However, it is rather general since it applies to many defect geometries and metallo-dielectric interfaces, and as will be shown, provides a simple insight into the physics of some important SP optical properties of these interfaces.

Section II is devoted to the electromagnetic study of the lamellar grating etched into metallic films, a classical one-dimensional geometry with many applications. Specifically, we study the physics of what will hereafter be called the isolated interface (the air-metal interface perforated by slits), and we introduce the electromagnetic quantities involved in the coupling mechanism between the incident plane wave and the fundamental Bloch mode supported by the slit array. To understand the complex SP-related phenomena of the isolated interface, we provide a thorough analysis of the poles and zeros of these electromagnetic quantities. Phenomena not reported before to our knowledge, like the resonance of the isolated interfaces at very small (but non-null) incidences and the possible absence of any reflection when outcoupling from an array of very narrow slits into free space, are found. In Sec. III, a perturbative approach allows us to provide a simple interpretation for these resonance phenomena and clearly evidences the complex role played by the SP waves. The symmetries of the grating geometry are shown to have a clear impact on the SP physics. In addition, we interpret the nearly null transmission recently predicted for these lamellar gratings[8] when the momentum of the incident wave matches the SP momentum of a flat interface (a phenomenon generally attributed to the Rayleigh anomaly, see Refs. 9 and 10, for instance) as a nonresonant SP effect. In Section 4, we illustrate the range of validity of the perturbative approach by studying other related structures, like metallic substrates perforated by slits, and metallic membranes perforated by two-dimensional arrays of holes. In addition, from the understanding gained with the perturbative approach, we engineer some other more complex one-dimensional structures for which SP effects may be controlled.

II. LAMELLAR GRATING

Perhaps the oldest example of metallic materials periodically corrugated by subwavelength defects is a metallic
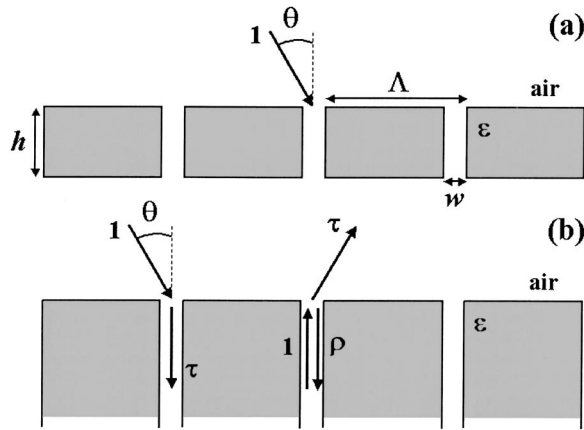
FIG. 1. (a) Diffraction by a lamellar grating under TM polarization. (b) Isolated single interface with the definition of the relevant electromagnetic quantities ρ and τ involved in the coupling between the zero-order and fundamental Bloch modes of the slit array.

membrane perforated by an array of slits; see Fig. 1(a) for a definition of the parameters of the structure. For microwave applications, the structure has been extensively studied for its polarization properties. A first comprehensive study of the resonance associated to cavity modes in the slits has been reported in Ref. 11 for perfectly conducting materials. Later on, anomalies of non-perfect metallic gratings with slit widths comparable to the wavelength have been studied theoretically[12] and numerically as well as experimentally.[13–16]

With recent advances in nanotechnology, there has been a renewed interest in the physical properties of metallic membranes perforated by an array of subwavelength slits.[8,17–21] Judging from that recent published literature, the physics, especially SP-related effects, of the coupling of light to the fundamental Bloch mode supported by the array of slits is not fully understood. For instance Treacy,[18] argues that SP play no casual roles in the transmission. Other authors[17,19–21] argue that the transmission at wavelengths close to the Rayleigh anomaly is enhanced by the excitation of coupled surface plasmons on the upper and lower interfaces of the metal grating. In Ref. 8, it is argued that SPs play a negative role in the transmission.

Throughout this section, we assume that the permittivity of the metal is $\varepsilon = (0.12 + 3.7i)^2$, independent of the wavelength. This approximation is inessential for the following discussion because we are mainly concerned with SP-related effects which are observed in a narrow energy band ($\Lambda < \lambda < 1.1\Lambda$). More importantly, this value of ε, which corresponds to the permittivity of silver at $\lambda = 0.7$ μm, avoids too close an energy proximity between SP and Rayleigh anomalies.[8] The numerical data are obtained with the improved version[22] of the rigorous coupled wave analysis (RCWA), an electromagnetic theory often used for analyzing grating diffraction.[23]

A. One-mode model

Virtually extending the slit region in Fig. 1(a) to infinity in both directions, we can consider the Bloch mode structure

of the slit array. It is well known that, when the slit is much smaller than the wavelength, only one Bloch mode propagates in the grating region, all the others being evanescent. In practice, this occurs approximately when $\lambda > 2w$.[11] The one-mode model[8,19,24,25] amounts to considering that the energy flow in the grating region is mediated only via the fundamental propagating Bloch mode. Within this approach, it is convenient to interpret the lamellar grating of Fig. 1(a) as two single interfaces perforated by an array of subwavelength slits. Figure 1(b) shows such an interface with the definition of the most relevant electromagnetic quantities, the coupling coefficient $\tau(\theta,\lambda)$ between the incident plane wave and the fundamental Bloch mode, and the reflection coefficient $\rho(\theta,\lambda)$ of this fundamental mode. In general, these quantities also depend on the permittivity for a given grating period and slit width. The mode and plane-wave expressions are normalized so that $|\rho|^2$ and $|\tau|^2$ represent the reflected and transmitted intensities. Analytical formulaes relying on approximate models based on surface impedance[19] or infinite conductivity[25] exist for these coefficients. However, because of the small conductivity of silver in the visible, these analytical formulaes are inaccurate in the SP energy band close to the Rayleigh anomaly. Thus, hereafter, we refer to exact electromagnetic computational results for $\rho(\theta,\lambda)$ and $\tau(\theta,\lambda)$ which are obtained with the RCWA. We emphasize that the electromagnetic response of the top and bottom interfaces is *rigorously modelized*, including any SP-related phenomena. From the knowledge of these coefficients, the zero-order transmission T of a lamellar grating of thickness h is straightforwardly obtained:

$$T = \left| \frac{\tau^2}{1 - |\rho^2|} \right|^2 \cdot \left| \frac{1 - |\rho^2|}{1 - \rho^2 \exp(2ik_0 n_{\text{eff}} h)} \right|^2 = \text{MT} \times \text{FP}, \quad (1)$$

where n_{eff} is the effective index of the fundamental Bloch mode propagating in the slit. Equation (1) is a standard Fabry-Perot formula that we have intentionally separated into two terms. The second term, labeled FP for Fabry-Perot, is related to the classical Airy resonance. Because $\text{Im}(n_{\text{eff}}) \ll 1$ for metals operating at optical frequencies, it can be set to 1 for arbitrary wavelength λ and angle of incidence θ provided that the grating depth h verifies the Fabry-Perot condition

$$k_0 \text{Re}(n_{\text{eff}})h + \arg(\rho) = m\pi, \quad (2)$$

where m is a signed integer. The first term, labeled MT, represents the *maximum transmission* that can be achieved for arbitrary h. Figure 2 shows the spectrum of all the relevant electromagnetic quantities for $\theta = 0°$. The solid dash dotted, and dashed curves in Fig. 2(a) show the calculated spectra of the MT, $|\rho|^2$ and $|\tau|^2$, respectively. Figure 2(b) shows the FP term as a function of h and λ. The maxima of FP are organized along four smooth curves. Every curve corresponds to a slit resonance according to Eq. (2), with different values of the integer m. We note that an abrupt change of the maximum of transmission along the spectrum appears when the wavelength is equal to the grating period. This is due to a sharp variation of the phase of the reflection coefficient ρ when the first orders of the isolated interface become propa-
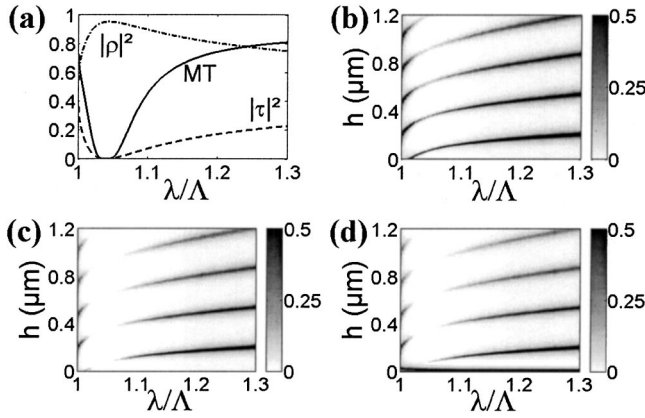
FIG. 2. Validation of the one-mode model for $\theta = 0°$. Parameters are $\varepsilon = (0.12 + 3.7i)^2$, $\Lambda = 0.7 \ \mu$m, and $w = 0.1 \ \mu$m. (a) Rigorously calculated spectra for MT (solid curve), $|\rho|^2$ (dash-dotted curve), and $|\tau^2|$ (dashed curve). (b) FP term as a function of λ and h. (c) One-mode model prediction (MT×FP) for the transmission. (d) Exact data for the transmission. A comparative inspection of (c) and (d) clearly shows that the model is highly accurate except for small depths.

gating (Rayleigh anomaly). Figure 2(c) shows the product MT×FP, obtained by multiplying the plot in Fig. 2(b) by the MT spectra [solid curve in Fig. 2(a)]. In Fig. 2(d) we represent exact numerical results obtained with the RCWA. Qualitatively, by comparing the plots of Figs. 2(c) and 2(d), it is obvious that the one-mode model reproduces the optical properties of the metallic membrane very well. Quantitatively, we found that, for any wavelength or incidence angle, the transmission predicted by the model and that computed with the RCWA never differ by more than 1% provided that $h > \lambda/3$. Physically, this thickness condition implies that the energy between the two single interfaces is mediated only via the fundamental propagating mode. This assumption, which is largely valid in previous related works,[8,17–21] will be used hereafter for understanding the optical properties of metallic membranes.

B. Poles and zeros of the isolated interface

It is well established nowadays that the anomalies or resonances of gratings can be understood with phenomenological studies, based on the computation in the complex plane of the poles and zeros of the scattering matrix; see Ref. 2 and references therein. For metallic membranes perforated by slits, this approach has been successfully applied to gratings with infinite conductivity[11] and more recently, to gratings with subwavelength slits.[21] With the hope to understand the role of SPs in the resonance transmission of such membranes, in this section we provide a thorough analysis of the poles and zeros of the electromagnetic quantities ρ and τ related to the coupling of the incident plane wave to the fundamental Bloch mode of the slit array. This is radically different from the approach in previous works,[11,21] which consisted of a study of the poles and zeros of electromagnetic quantities related to the full problem, like the membrane transmission T. We emphasize that *the resonances of the single interface are not the resonances of the full problem.* For instance, the poles of ρ and T are different, as evidenced by Eq. (1).

1. Zero of τ

As shown in Fig. 2(c), the transmission of the metallic membrane is nearly zero in the SP energy band ($\lambda = 1.03 \ \Lambda$) for arbitrary depth. This is a general property of such membranes: extremely weak transmissions ($<10^{-6}$) for arbitrary h, θ, and ε are achieved whenever the momentum of the incident wave matches the SP momentum of a flat interface modulo the grating vector,[8] i.e., for wavelengths λ_{sp} given by

$$\lambda_{sp} = \frac{\Lambda}{m} \left\{ \text{Re} \left[\left(\frac{\varepsilon}{1 + \varepsilon} \right)^{1/2} \right] \pm \sin(\theta) \right\}, \quad (3)$$

with m a nonzero signed integer. This phenomenon, which must not be confused with the Rayleigh or Wood anomalies, is due to the existence of a nearly real zero for τ for $\lambda \approx \lambda_{sp}$, as exemplified by the dashed curve in Fig. 2(a) (which corresponds to the specific case $\theta = 0°$). According to Eq. (1), the spectral dependence of the membrane transmission T can be expected to vary as $T \approx (\lambda_{sp} - \lambda)^4$, resulting in a low and flat transmission over a broad spectral range. Since the existence of this zero has previously attracted much attention,[8] it is not necessary to comment further on this phenomenon which will be understood as a nonresonant SP effect in Sec. III.

2. Poles of ρ and τ

Electromagnetic calculations of the complex photonic band structure of a single isolated interface have been carried out with the RCWA by computing the poles β (complex value of the normalized parallel momentum) of ρ and τ. These poles are the same since they correspond to the singularities of the determinant of the scattering matrix.[2] Figure 3(a) shows the spectra of Re(β) and Im(β). Concerning the real part of β, it is found that the SP-resonance dispersion relation of the single isolated interface nearly corresponds to that of a flat air-metal interface, whose Re(β) is represented by circles. More remarkable is the deep minimum of Im(β) observed for $\lambda \approx 1.03\Lambda$. The corresponding value for Re(β) is $\theta = 0.7°$. As shown in Fig. 3(b), this minimum reflects in the diffraction problem associated to a 700-nm-thick membrane. For $\lambda \approx 1.03\Lambda$, a strong absorption peak (dotted curve) is observed for $\theta = 0.7°$. This peak, which mainly corresponds to a resonance of the upper grating surface, does not show up in the absorption spectrum for $\theta = 0°$ (solid curve), for which only one peak related to the slit resonance [pole of the transmission T in Eq. (1) according to Eq. (2)] is observed for $\lambda/\Lambda \approx 1.1$. We also computed the reflected negative r_{-1} and positive r_{+1} first-order amplitudes diffracted by the 700-nm-thick membrane with the RCWA. The phase origin for r_{-1} and r_1 is chosen in the mirror symmetry plane in the center of the slit. Figure 3(c) shows the ratio $\alpha = |r_{-1} + r_{+1}|/(|r_{+1}| + |r_{-1}|)$ as a function of the normalized wavelength. As could be expected from symmetry consider-
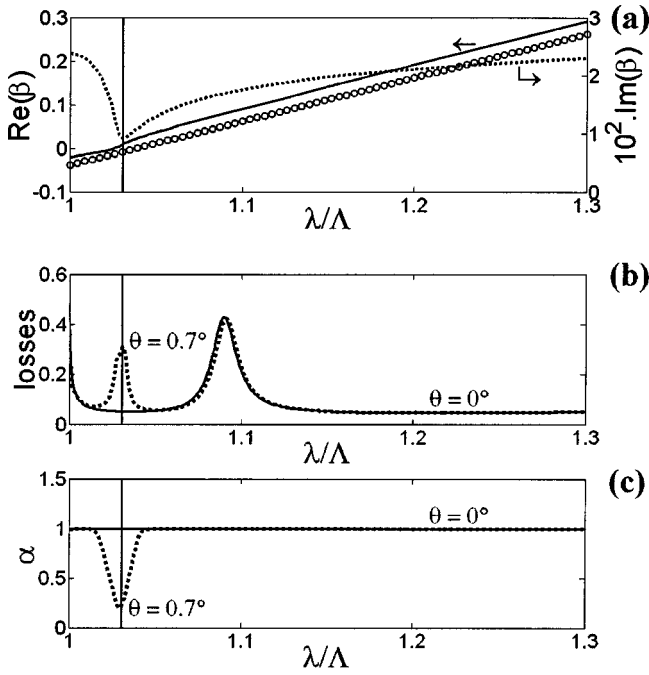
FIG. 3. Resonance of the single isolated interface. (a) Spectral dependence of the complex momentum pole β (solid curve: real part; dotted curve: imaginary part) of the single interface of Fig. 1(b). Circles represent the SP dispersion of a flat interface according to Eq. (3). (b) Absorption of a 700-nm-thick membrane for $\theta=0°$ (solid curve) and for 0.7° (dotted curve). The absorption peak for $\lambda\approx1.1\ \Lambda$ is due to the resonance of the slit. The corresponding peak transmission is small, $\approx8\%$. The peak for $\lambda\approx1.03\ \Lambda$, observed only for $\theta=0.7°$, is due to the SP resonance on the two grating lower and upper interfaces. The corresponding transmission ($\approx1.5\%$) is very weak. (c) Evidence of the presence of an antisymmetric SP pattern for the resonance at $\theta=0.7°$. α is the normalized sum of the positive and negative first reflected orders of the 700-nm-thick membrane. Grating parameters are the same as in Fig. 2.

ations, the solid curve ($\theta=0°$) shows that r_{-1} and r_1 are in-phase ($\alpha=1$) for any wavelength. In addition we noted that r_1 (or r_{-1}) is small (≈1) over the full spectrum including wavelengths corresponding to the absorption peak for $\lambda/\Lambda\approx1.1$. The dotted curve, which holds for $\theta=0.7°$, is similar except that a strong minimum is observed for $\lambda\approx1.03\Lambda$. For this minimum, r_{-1} (or r_1) is large (≈13), showing the resonant nature of the phenomenon. As will be explained in Sec. III the minimum for α is due to the resonant excitation of two counterpropagating SPs with opposite amplitudes on the isolated interface.

3. Zero of ρ

Because the fundamental mode supported by the slit is a propagating one, the energy conservation law imposes that the reflection coefficient ρ presents a complex zero in the close proximity of its pole.[2] Using the RCWA, we calculated the complex zeros of ρ for the single interface. We found that this zero is *nearly real* for $\theta=0.92°$ and $\lambda=1.03\Lambda$, a value very close to $\theta=0.7°$ (SP resonance). According to Eq. (1), a real zero implies that the transmission of the air membrane is nearly independent of the grating thickness provided that
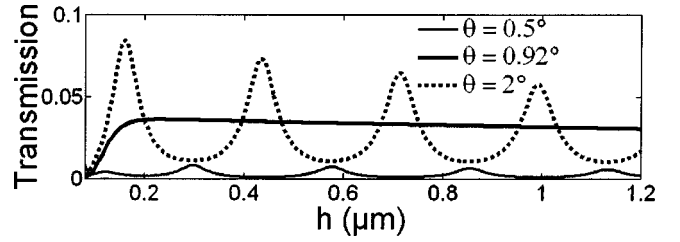
FIG. 4. Transmission of the lamellar grating vs its depth showing the absence of any reflection when outcoupling from an array of very narrow slits into free space. The bold curve, achieved for $\theta=0.92°$, shows a grating transmission nearly independent of the grating depth. The two other curves correspond to $\theta=2°$ and $\theta=0.5°$. Other parameters are $\Lambda=1.03\ \Lambda$, $\varepsilon=(0.12+3.7i)^2$, $\Lambda=0.7\ \mu$m, and $w=0.1\ \mu$m.

$\mathrm{Im}(n_{\mathrm{eff}})\ll1$. As shown by the bold curve in Fig. 4, this prediction is confirmed by rigorous computational results. For $h>0.2\ \mu$m, a transmission of 4% is obtained, independently of the grating thickness. This low value for the transmission is due to the momentum proximity with the null-transmission at λ_{sp}. In this phenomenon which is indeed related to SP excitations on the top and bottom grating interfaces, SPs act as antireflection coatings for the channel. Consequently, the energy flows unidirectionnaly in the structure. The reflected zero-order intensity ($\approx66\%$) is also independent of the grating depth, a large fraction ($\approx30\%$) of the energy being absorbed on the grating interfaces.

III. PHYSICAL PICTURE: PERTURBATIVE APPROACH

In this section, we present a perturbative approach that provides a simple interpretation for the phenomena discussed in Sec. II. Within this approach, we interpret the zero of τ as a nonresonant SP effect and the absorption anomaly at $\lambda=1.03\Lambda$ in Fig. 3(b) as the exaltation on the isolated interface of two resonant counterpropagating SPs with opposite amplitudes.

Let us first consider a plane interface between a metal and a dielectric material, with relative permittivities ε and ε', respectively. In the presence of an incident plane wave with unit amplitude at frequency ω, the unique solution of Maxwell's equations consists of one reflected wave and one transmitted waves with amplitudes r and t, the complex Fresnel coefficients. In the absence of external excitation, SP waves confined at the interface exist. For a given frequency ω, their parallel momentum k_{sp} is simply[1] $k_{sp}=(\omega/c)\sqrt{\varepsilon\varepsilon'/(\varepsilon+\varepsilon')}$. From these solutions, a set of linear combinations for which the magnetic field is periodically null at the interface can be readily exhibited for TM polarization. Two of them are shown in Figs. 5(a) and 5(b). In Fig. 5(a), the electromagnetic field consists in an incident plane wave with the associated reflected and transmitted waves and a SP wave propagating either in the left or in the right direction with an amplitude of $-(1+r)$ at the interface. The magnetic field H on the interface is thus

$$H(x)=(1+r)\{\exp[jk_0\sqrt{\varepsilon'}\sin(\theta)x]-\exp(\pm jk_{sp}x)\},$$

$$(4)$$
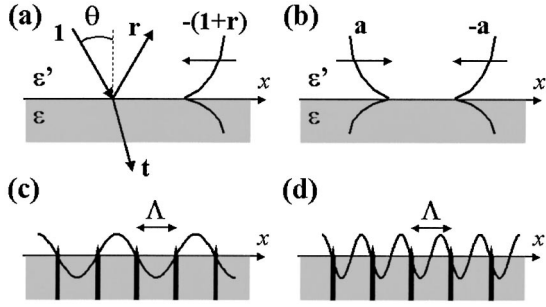
FIG. 5. Two solutions of Maxwell's equations for a metallodi-electric flat interface which provide a periodically null field at the interface, with a periodicity constant Λ given by Eqs. (5) and (7). (a) Solution in the presence of an incident plane wave. (b) Solution in the absence of external excitation. (c) Field pattern associated to (a). (d) Field pattern associated with (b). In (c) and (d) the origin of the null field is placed on the interface, and the dark pins represent subwavelength defects that could be introduced without much perturbating the field patterns.

with $k_0 = \omega/c$. It is easily shown that, if one neglects the SP attenuation along the interface, Eq. (4) provides a periodically-null pattern on the interface with a periodicity constant Λ given by

$$ m\frac{\lambda}{\Lambda} = \pm \mathrm{Re}\left[\left(\frac{\varepsilon\varepsilon'}{\varepsilon+\varepsilon'}\right)^{1/2}\right] - \sqrt{\varepsilon'}\sin(\theta), \quad (5) $$

m being a nonzero signed integer. For small incidences, the solution for a null-field pattern degenerates into a normally incident plane wave and two counterpropagating SPs with equal amplitudes $-(1+r)/2$, the magnetic field H on the interface being $(1+r)\,[1-\cos(k_{sp}x)]$. The second linear combination [see Fig. 5(b)] is simply the superposition of two counterpropagating SP waves with opposite arbitrary amplitudes a and $-a$. Thus the magnetic field H on the interface is simply

$$ H(x) = a[\exp(+jk_{sp}x) - \exp(-jk_{sp}x)], \quad (6) $$

which provides a periodically null-field pattern, if one neglects the SP attenuation along the interface. The periodicity constant of this pattern is given by

$$ m\frac{\lambda}{\Lambda} = \mathrm{Re}\left[\left(\frac{\varepsilon\varepsilon'}{\varepsilon+\varepsilon'}\right)^{1/2}\right]. \quad (7) $$

Note that the condition of Eq. (7) simply corresponds to $\theta = 0°$ in Eq. (5). Equations (5) and (7) are classical since they can be read as phase matching conditions between an incident plane wave and the SP momentum of a flat interface through a grating momentum $2\pi/\Lambda$. However, let us emphasize that in the present approach, they simply represent conditions such that a periodically-null solution of Maxwell's equations with a period Λ exists on a flat interface for TM polarization. No grating and no phase matching have been considered for their derivation.

In a perturbative approach, one intuitively expects that these two solutions of Maxwell's equations remain valid if an array of subwavelength defects, like etches or particles

[represented by dark pins in Figs. 5(c) and 5(d)], are incorporated at the periodically null-field locations. Within this approach, we now explain the nearly-null transmission and the resonance observed in Fig. 3 for very small, but non null, incidences.

A. Explanation for the zero of τ

We claim that the solution of Maxwell's equations represented in Fig. 5(a) remains essentially valid for the metallic membrane of Fig. 1(a) provided that the periodicity constant of the grating corresponds to the periodicity constant of the null-field pattern. In the problem we consider, Λ and ε are given. Thus Eq. (5) gives the set of wavelengths λ and angles of incidence θ for which the magnetic field on the grating presents a null-field pattern. For these parameters, the corrugated surface will behave almost as a flat one, with nearly the same reflectance $|r|^2$ and absorption $1-|r|^2$. In other words, the incident light does not "see" the array of subwavelength defects and, consequently, no energy can be transferred into the fundamental slit mode: τ is null. This is effectively what was observed in Sec. II B. In addition, we checked through additional rigorous computations that, whenever the parallel momenta of the SP of a flat interface and of the incident wave are matched modulo the grating vector, the intensity of the zero order reflected by the lamellar grating is nearly equal to that of a flat interface. For instance, for $\theta = 0°$ and for $\lambda = \lambda_{sp}$, the intensities reflected in the zeroth order vary between 0.95 and 0.958 for $h > \lambda/5$, to be compared to the reflectance of a flat interface $|(\varepsilon^{1/2}-1)/(\varepsilon^{1/2}+1)|^2 = 0.968$. The slight difference is due to the fact that the SP launched onto the interface slightly dissipates. Thus within the perturbative approach, the nearly-real zero for τ for $\lambda = \lambda_{sp}$, which results in a nearly null transmission for the lamellar grating, is interpreted as a nonresonant SP effect.

B. Explanation for the pole of ρ

The linear combination shown in Fig. 5(b) offers radically different perspectives. It corresponds to a leaky wave which approximately satisfies Maxwell's equations for the corrugated interface in the absence of external excitation, provided that the periodicity constant of the corrugations corresponds to that of the null-field pattern given by Eq. (7). In the absence of corrugations (flat interface), the linear combination represents a purely bound guided wave, but by introducing subwavelength periodic defects, this wave weakly interacts with the defects, becomes leaky and radiates in some space harmonics. Excited with an external source, like a plane wave with unit amplitude impinging at the same angle as would be taken by the leaky wave orders, a resonance can be excited: the resonance field will correspond to a strong SP sinusoidal pattern ($a \gg 1$) with a weak superimposed background.

Let us now discuss the phase-matching condition for this resonant excitation. Optimal excitation of two counterpropagative SPs on a grating requires normal incidence. For $\theta = 0°$, the two SP momenta can be exactly matched through the reciprocal grating vectors $2\pi/\Lambda$ and $-2\pi/\Lambda$; see Fig. 6(a). However, because the grating considered in this work
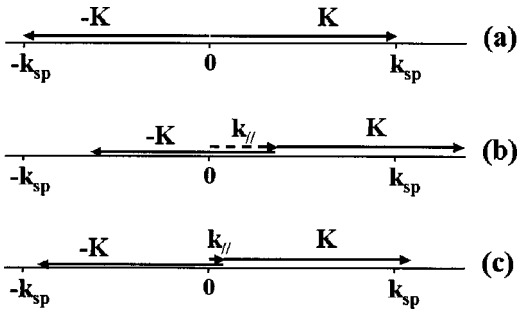
FIG. 6. Phase matching condition for the excitation of two counterpropagative SPs with opposite amplitude. (a) For normal incidence, the two SP momenta are perfectly matched through the grating momentum but, for a grating with a vertical mirror symmetry, the SPs have equal amplitudes. (b) For oblique incidence, the phase matching condition is not satisfied. (c) For small incidence angles, the phase matching is nearly satisfied and counterpropagative SPs with opposite amplitudes can be excited even for a grating with a mirror-symmetry. $k_\parallel$ denotes the parallel component of the incident wave vector.

FIG. 7. SP-related effects on subwavelength lamellar grating etched into a metallic substrate. (a) Grating geometry. (b) Absorption spectrum for $\theta=0°$. (c) Absorption spectrum for $\theta=0.7°$. Vertical dashed lines represent frequencies for which a zero of τ is predicted according to Eq. (5). Grating parameters are the same as in Fig. 2.

has a mirror symmetry along the vertical axis passing by the slit center, the amplitudes of the reflected positive- and negative-first orders in this plane are strictly equal under normal incidence, as observed in Fig. 3(c). Thus, for $\theta=0°$, only counterpropagative SPs with equal amplitudes can be excited. Actually, this situation corresponds to the nonresonant SP pattern responsible for the zero of τ under normal incidence. To excite counterpropagative SPs with opposite amplitudes, one has to brake the symmetry. One possibility is to consider gratings without the mirror symmetry, as will be discussed in Sec. III. Another possibility is to illuminate the lamellar grating under oblique incidence. For rather large values of θ, one intuitively expects that the antisymmetric SP pattern will not be excited efficiently because of the strong momentum mismatch; see Fig. 6(b). However, as illustrated in Fig. 6(c) for very small θ values the momentum matching condition approximately holds, the mirror symmetry is broken and the antisymmetric SP resonance could be efficiently excited. As shown in Fig. 3, we found that this resonant excitation holds for $\theta=0.7°$ for the permittivity and slit width considered in this work.[26] Although not strictly equal to zero because $|r_{+1}|\neq|r_{-1}|$ at oblique incidence, *the minimum for α in Fig. 3(c) clearly evidences the presence of two counterpropagating SPs with opposite amplitudes.*

In general, the absolute value of the imaginary part of a complex pole of a scattering matrix is related to the impact of this pole in real experiments with real values of β.[2] The larger Im(β) is, the less spectacular the consequence of the pole in experiments. With this in mind, we are now able to interpret the strange behavior for the imaginary part of the pole of ρ in Fig. 3(a). For $\theta<0.7°$, i.e., on the left side of the dip in Fig. 3(a), Im(β) quickly increases because of the symmetry of the diffraction problem which does not allow for the excitation of counterpropagative SP with opposite amplitudes. For $\theta>0.7°$, i.e., on the right side of the dip in Fig. 3(a), the phase matching condition for two counterpropagative SPs is less and less satisfied when λ increases (see Fig. 6), and consequently Im(β) slowly increases.
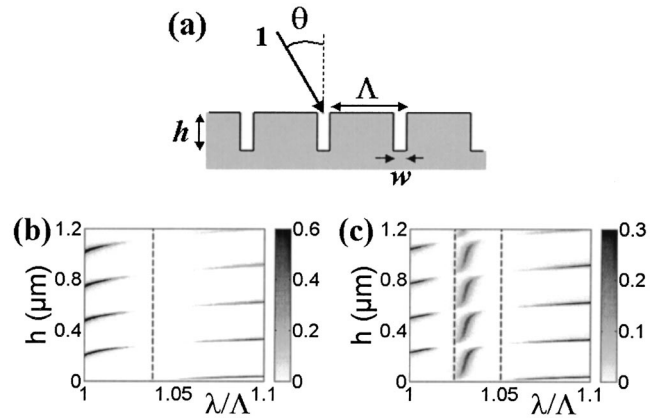
IV. OTHER RELATED GRATING GEOMETRIES

As we have seen, the perturbative approach based on building up linear combinations of Maxwell's solutions for the flat interface well explain the complex SP-related phenomena of lamellar gratings etched into metallic films. The objective of this section is to show that the approach is general, since it applies as well to other related one- and two-dimensional periodic structures. In addition, we show how the perturbative approach of Fig. 5 can be useful for engineering the optical response of metallic grating structures.

A. Subwavelength lamellar grating etched into a metallic substrate

The slit resonance of subwavelength lamellar gratings etched into a metallic substrate; see Fig. 7(a) for the definition of the grating parameters, were recently studied theoretically[27] as well as experimentally.[28] The optical response of these gratings can be studied with the one-mode model of Sec. II. This response being qualitatively very similar to those of subwavelength lamellar gratings etched into metallic films, hereafter we only present the main features for the sake of conciseness.

Figures 7(b) and 7(c) show the absorption losses computed with the RCWA for $\theta=0°$ and $0.7°$, respectively. In view of the previous analysis, the interpretation of these spectra is simple. The background fringe pattern is due to slit resonance for Fabry-Perot conditions $2k_0 \mathrm{Re}(n_{\mathrm{eff}})h+\arg(\rho)+\arg(\rho_1)=2m\pi$, where ρ_1 is the modal reflectivity coefficient on the bottom grating interface. The slit no longer resonates when the nonresonant SP pattern responsible for the zero of τ is excited, i.e., for wavelengths $\lambda_{sp}=\Lambda \mathrm{Re}[\varepsilon/(\varepsilon+1)]^{1/2}$ in Fig. 7(b), and $\lambda_{sp}=\Lambda\{\mathrm{Re}[\varepsilon/(\varepsilon+1)]^{1/2}\pm\sin(\theta)\}$ in Fig. 7(c), represented by vertical dashed lines. In addition, we note that, in Fig. 7(c), a strong absorption nearly independent of the grating depth is observed in the spectral region delimited by the two vertical lines. From the previous

(a)

(b)

(c)

(d)
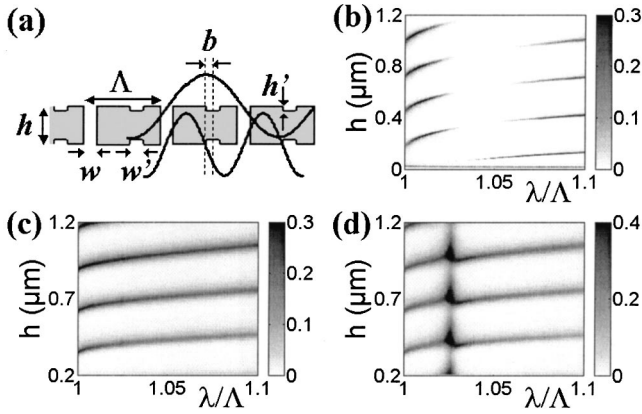
FIG. 8. Engineered one-dimensional gratings. (a) Grating geometry. For $b=0$, the grating structure possesses a vertical-mirror symmetry. (b) Absorption spectrum for $b=0$ and $h'=0$ (lamellar grating studied in Sec. II). (c) Absorption spectrum for $b=0$. (d) Absorption spectrum for $b=\Lambda/35$. Other parameters are $\varepsilon=(0.12+3.7i)^2$, $\Lambda=0.7$ μm, $w=0.1$ μm, $\theta=0°$, $h'=0.1$ μm, and $w'=40$ nm.

analysis, this phenomenon is readily interpreted as the resonance of the antisymmetric SP pattern on the upper grating boundary.

B. Engineered one-dimensional gratings perforated by subwavelength slits

Let us consider the grating shown in Fig. 8(a). In comparison with Fig. 1(a), two additional subwavelength slits of finite depth h' have been added on the upper and lower grating interfaces. The parameter b denotes the horizontal shift of the additional slits with respect to the middle of the ridge. For $b=0$, the grating possesses a vertical-mirror symmetry. In Fig. 8(a), we have represented the field pattern of the nonresonant SP (top interface) and that of the resonant antisymmetric SP (bottom interface). Null field locations are represented on the interfaces. Clearly, one sees that the nonresonant SP pattern is no longer solution of the engineered isolated interface, since the field is not null on the additional subwavelength slit (it is even maximum at this location). On the contrary, the resonant SP pattern composed of two counterpropagative SPs with opposite amplitudes remains a solution of Maxwell's equations of the engineered isolated interface since the additional slits are etched on the null-field locations.

With these facts in mind, we are able to interpret the absorption spectra of Figs. 8(c) ($b=0$) and 8(d) ($b=\Lambda/35$) calculated for normal incidence with the RCWA. For the sake of comparison the absorption spectrum for the grating of Sec. II (i.e. for $h'=0$) is represented in Fig. 8(b). As expected qualitatively, it is found that the fringe pattern due to the slit resonance is not interrupted for $\lambda=\lambda_{sp}$ in Fig. 8(c). Because the nonresonant SP pattern responsible for a zero of τ is no longer a solution of Maxwell's equation, the slit can resonate, even when the parallel momenta of the SPs of a flat interface and of the incident-wave are matched. The absorption spectrum of Fig. 8(d) obtained for a grating with

a very small dissymmetry ($b=\Lambda/35$) offers a strong resonance for $\lambda\approx1.03\Lambda$ and for arbitrary depths. This resonance is due to the counterpropagative SP pattern which can be highly excited under normal incidence for this nonsymmetric grating structure.

C. Two-dimensional gratings perforated by subwavelength apertures

Recently, metallic membranes perforated by a two-dimensional array of subwavelength holes have received much experimental[5,9,29] and theoretical[10,30,31] attention because the transmission of light through these membranes can be up to 2–3 orders of magnitude larger than that predicted by the conventional aperture theory. For these membranes, it has been shown that, for deep enough gratings, the energy transfer through the membrane is mainly driven by one specific evanescent mode[10,30] and that a one-mode model provides a good qualitative explanation of the physics of the remarkable transmission[10] through a pole of ρ. Undoubtedly, providing a physical picture with a perturbative approach (as we did in Sec. III for lamellar one-dimensional gratings) which explains the existence of this pole would be beneficial for the understanding and for applications. We were not able to provide such a physical picture probably because the pole responsible for the remarkable transmission corresponds to the existence of an intense field pattern inside the hole and in the vicinity of the hole, which cannot be obtained at with SP patterns with a periodically-null field on the hole. Thus, our intention in this Section is to show that the perturbative approach developed in Sec. III remains valid for the two-dimensional case. The result is an overall better understanding of the SP-related phenomena in these membranes.

1. Zero of τ

In this subsection, we aim at deriving superpositions of plane waves and SP waves which are periodically null on a flat metallo-dielectric interface. Although the discussion can be set in general terms, we assume in the following that the periodic null pattern is a square lattice with a periodicity constant Λ in the x and y directions. Let us denote by **G** the reciprocal lattice vector of the periodic null pattern, $\mathbf{G}=2\pi/\Lambda(m\mathbf{x}+n\mathbf{y})$, with m and n signed integers.

Let us consider that the flat interface is illuminated by an incident plane wave with a given wavelength λ in a vacuum, and let us denote by $\mathbf{k}_\parallel$ the parallel component of the incident wave vector and by $\mathbf{H}_\parallel$ the parallel component of the magnetic-field vector. The frequency of the wave being given, the modulus k_{sp} of the SP wave vector to be considered for the linear superposition is fixed. In general, a periodically null field pattern is achieved by the superposition of the incident plane wave, of the reflected plane wave and of a single SP, wave provided that

$$\mathbf{k}_\parallel+\mathrm{Re}(\mathbf{k}_{sp})=\mathbf{G}, \tag{8}$$

and that

$$\mathbf{k}_{sp}\cdot\mathbf{H}_\parallel=0. \tag{9}$$
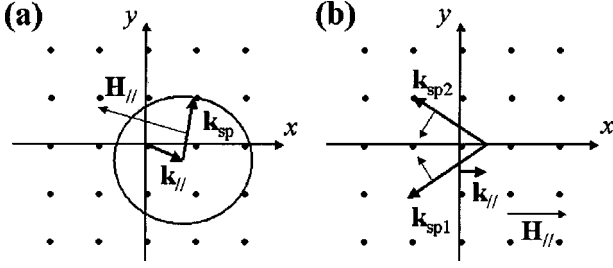
FIG. 9. SP configuration providing a null field pattern in the presence of an incident plane-wave, on a square lattice of periodicity constant Λ in the x and y directions. Dots represent the reciprocal lattice vectors **G**. $\mathbf{k}_\parallel$, and $\mathbf{H}_\parallel$ are the parallel components of the wave vector and of the magnetic field of the incident plane wave. (a) General scheme; note that $\mathbf{k}_{sp}$ and $\mathbf{H}_\parallel$ have to be orthogonal. (b) Specific case with two SP waves and with an incident plane wave with a transverse-electric polarization.

Equation (9) can be read as a polarization selection condition. This general situation is depicted in Fig. 9(a) for the specific case $\mathbf{G}=2\pi/\Lambda$ $(\mathbf{x}+\mathbf{y})$. The demonstration is straightforward. Let us denote by ρ the in-plane vector ($x\mathbf{x}+y\mathbf{y}$). For the linear combination formed by the incident plane wave, the associated reflected plane wave and a SP wave with a magnetic field $-(1+r)\mathbf{H}_\parallel$, the total parallel magnetic field $\mathbf{H}_p$ on the flat interface is then

$$\mathbf{H}_p = \mathbf{H}_\parallel (1+r)[\exp(j\mathbf{k}_\parallel \cdot \rho) - \exp(j\mathbf{k}_{sp} \cdot \rho)]. \quad (10)$$

As previously done for the one-dimensional case, if ones neglects the SP wave attenuation, we deduce from Eq. (10) that $\mathbf{H}_p$ is periodically null on the lattice node. For the sake of convenience hereafter, Eq. (8) can be rewritten

$$(\sqrt{\varepsilon'} \sin(\theta)\cos(\delta) - m\lambda_{sp}/\Lambda)^2$$
$$+ (\sqrt{\varepsilon'} \sin(\theta)\sin(\delta) - n\lambda_{sp}/\Lambda)^2$$
$$= \left\{ \mathrm{Re}\left[\left(\frac{\varepsilon\varepsilon'}{\varepsilon + \varepsilon'} \right)^{1/2} \right] \right\}^2, \quad (11)$$

where θ denotes the angle of incidence of the plane wave and δ the angle between the x axis and the plane of incidence. Thus for a given geometry, Eq. (11) provides the set of wavelengths λ_{sp} for which the linear combination is null periodically. Note that Eq. (11) represents a necessary condition for the observation of a weak transmission, which is not sufficient since the polarization selection condition of Eq. (9) also has to be satisfied.

Of special interest are geometries for which several SPs can be involved in the linear combination. Figure 9(b) shows the situation for which $\mathbf{k}_\parallel \cdot \mathbf{y}=0$ and $\mathbf{H}_\parallel \cdot \mathbf{y}=0$ (transverse-electric polarization) and a coupling through the reciprocal vectors $\mathbf{G}=2\pi/\Lambda$ $(-\mathbf{x}\pm\mathbf{y})$. For normal incidence, four SP waves can be involved in the linear combination.

From the previous analysis, it is predicted that when the momentum of the incident wave matches the SP momentum of a flat interface through the grating momentum wavevector according to Eqs. (8) or (11), the optical response of a metallic membrane perforated by subwavelength apertures is
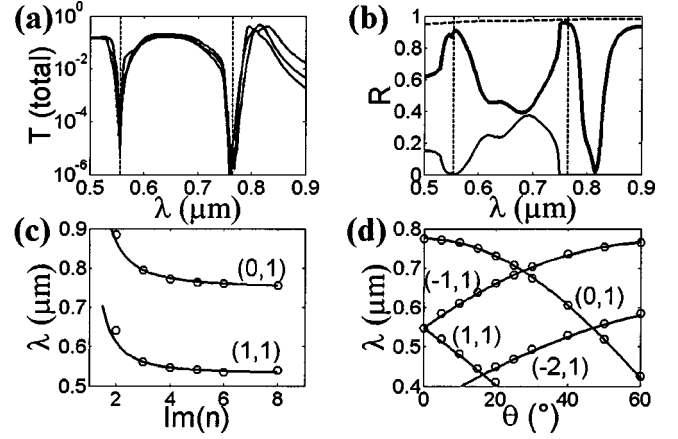
FIG. 10. Zeros of τ for metallic membranes in air perforated by a two-dimensional array of subwavelength square holes ($\Lambda = 0.75$ μm). (a) Calculated transmission spectra of silver gratings for three different grating depth $h=320$, 400, and 500 nm and for $\theta=0°$. Two dips in the transmission curves are observed for $\lambda = \lambda_{sp}$ (vertical dashed lines). (b) Silver grating reflectance spectra for $\theta=0°$ and for $h=400$ nm. Bold curve: specular reflectance. Thin curve: non-specular reflectance. Dashed curve: reflectance of an air-silver interface. For $\lambda = \lambda_{sp}$ (vertical dashed lines), the grating nearly behaves as a flat interface. (c) Null transmission for gratings with different permittivity, $\varepsilon = (0.1 - in'')^2$ with $2 < n'' < 8$, and illuminated under normal incidence. (d) Oblique incidence with $\mathbf{k}_\parallel$ parallel to the x axis and a transverse-electric polarization, [see Fig. 9(b)], and for a metal with a refractive index $0.1-4i$ independent of the wavelength. In (c) and (d), circles correspond to wavelengths $\lambda_{\min}$ for which the calculated transmission spectra present a very weak transmission ($<10^{-4}$) and solid curves are λ_{sp} wavelengths computed from Eq. (11) for the set of (m,n) values indicated in the figures. A very good agreement is obtained.

nearly that of a plane metallodielectric interface. As was done previously for one-dimensional gratings,[8] we have checked this property with many numerical computations performed with the Fourier modal method[32] for metallic membrane in air perforated by a two-dimensional array ($\Lambda = 750$ nm) of square holes of size 280 nm. This specific geometry has been previously studied in great details.[10] The main results are summarized in Fig. 10.

Figures 10(a) and 10(b) are relative to silver gratings illuminated under normal incidence. In Fig. 10(a), the total transmission spectrum is shown for three grating depth $h = 320$, 400, and 500 nm and for $\theta=0°$. For $\lambda\approx 800$ nm, a transmission as large as $\approx 50\%$ is computed in agreement with previous numerical and experimental results.[10] According to the previous analysis, a very small transmission ($\approx 10^{-5}$) is predicted for the three different depths and for wavelengths given by Eq. (11), represented by the two dashed vertical lines in the figure. Figure 10(b) shows the reflectance spectra of the grating for $\theta=0°$ and $h = 400$ nm. The bold curve represents the specular reflectance in the (0,0)th order. The thin curve represents the non-specular reflectance, i.e., the intensity reflected in all orders except in the (0,0)th one. For $\lambda = \lambda_{sp}$ (vertical dashed lines), it is remarkable that the grating behaves as a flat interface: the non-specular reflectance is nearly zero, the transmission

is nearly zero [see Fig. 10(a)], and the specular reflectance is close to that of an air-silver interface (dashed curve), a residual absorption being carried out by the excitation of the nonresonant SP pattern.

Figure 10(c) is relative to metallic gratings with different permittivity values defined by $\varepsilon = (0.1 - in'')^2$ with $2 < n''$ < 8 and illuminated under normal incidence. The circles correspond to wavelength λ_{min} for which we observed a very small transmission from transmission spectra calculated with the RCWA for $\theta = 0°$. The bold curves are λ_{sp} wavelengths computed with Eq. (11) for $(|m|, n) = (1,0)$ and $(|m|, |n|)$ $= (1,1)$. Except for $n'' = 2$, λ_{min} almost coincides with λ_{sp}. Within the perturbative model, the weak disagreement for $n'' = 2$ can be understood by the fact that the SP attenuation can no longer be neglected for metals with small conductivities. Figure 10(d) corresponds to oblique incidence with $\mathbf{k}_\parallel$ parallel to the x axis and a transverse-electric polarization. Again the circles correspond to wavelength λ_{min} for which we observed a very small transmission from transmission spectra calculated with the RCWA for different angles of incidence, $\theta = 0°$, $5°$, $10°$ ...$60°$ and for a metal with a refractive index $0.1 - 4i$ independent of the wavelength. These wavelengths are in very good agreement with the λ_{sp} values given by Eq. (11) [solid curves in Fig. 10(d)].

The null transmission of metallic membranes perforated by subwavelength holes has been largely attributed to Rayleigh anomalies in the literature, see Refs. 5, 9, and 10 and references therein. From the present analysis, it is concluded that the null transmission is a very general property of two-dimensional metallic gratings with subwavelength apertures and that it is due to the nonresonant excitation of SPs.

2. Pole of ρ

As we did for one-dimensional gratings, we look for superpositions of SP waves which are periodically null on a flat metal-dielectric interface. Figure 11(a) shows such superpositions in the reciprocal space when the SP wave-vector modulus is equal to $2\pi/\Lambda$. Configurations (1) and (2) are relative to two SP waves with opposite amplitudes which are propagating along the y and x axes, respectively. They are strictly identical to the SP pattern discussed in Sec. III for the one-dimensional case. For the two-dimensional case, because of the huge amount of computation required, we have not extensively studied by calculations the spectral behavior of the poles of ρ. Nevertheless, to verify the possibility of exciting for very small incidences two counterpropagating SP waves, we simply compute the losses associated to silver membranes for $h = 400$ nm and for some arbitrary small angle of incidence, $\theta = 0.7°$. Note that this value that was identified as pecular for the one-dimensional lamellar grating is absolutely arbitrary for the two-dimensional case.

Figure 11(b) shows the absorption losses of the silver membrane for $\theta = 0°$, and for $\theta = 0.7°$, $\delta = 0°$, and two different polarizations. Vertical lines are λ_{sp} values given by Eq. (11) for $\theta = 0.7°$. Note that Eq. (11) can be read in two different ways: as a condition for observing a null transmittance [it is the case if Eq. (9) is satisfied], or as a phase-matching condition for the excitation of two counterpropagating SPs under slight oblique incidence. The spectra are
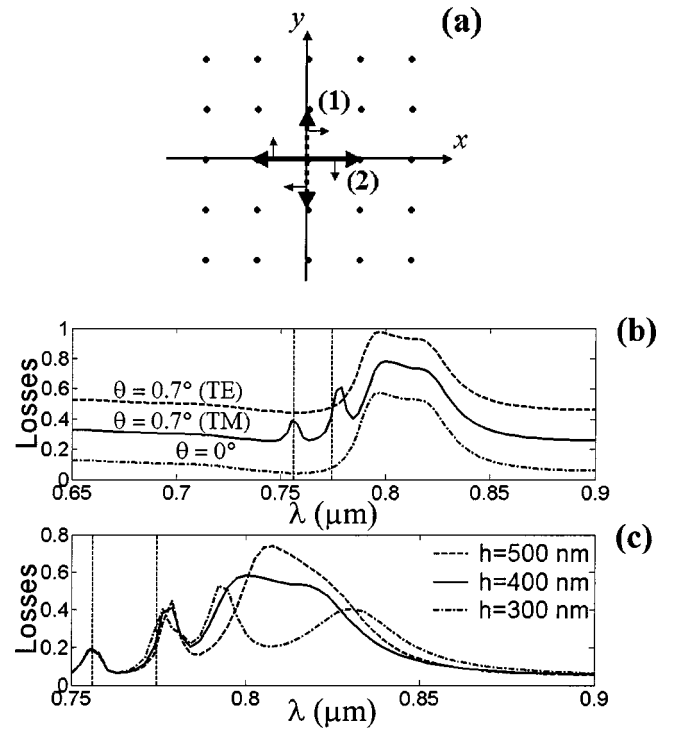
FIG. 11. Counterpropagating SP with opposite amplitude on a metallic silver membrane. (a) SP configurations with $k_{sp} = 2\pi/\Lambda$ providing a null field pattern on a square lattice of periodicity Λ in the x and y directions in the absence of incident illumination. Configurations (1) and (2) are relative to two SP waves propagating along the y and x axes, respectively. Dots represent the reciprocal lattice vectors and the thin vectors the magnetic polarization of the SP waves. (b) Absorption losses of a silver grating for $\theta = 0°$, $\theta = 0.7°$, and for different polarizations. Vertical dashed lines are λ_{sp} values given by Eq. (11). The spectra are vertically shifted by 0.2 for the sake of clarity. (c) Absorption losses of a silver grating for $\theta = 0.7°$, $\delta = 0°$, and TM polarization and for different grating depths. The losses associated with the hole resonance (for $\lambda \approx 0.8 \mu$m) strongly depend on the grating depths, whereas the losses associated with the resonant excitation of counterpropagative SPs with opposite amplitudes do not.

vertically shifted by 0.2 for the sake of clarity. Under normal incidence, the SP pattern of Fig. 11(a) cannot be excited and the large and intense peak at $\lambda \approx 0.8 \mu$m is due to the hole resonance associated to the extraordinary transmission. For $\theta = 0.7°$ and for TM polarization, two additional peaks are observed for λ_{sp} wavelengths given by Eq. (11). These peaks are easily interpreted by the excitation of the SP pattern (2) in Fig. 11(a). SP pattern (1) cannot be excited because of the mirror symmetry along the x axis of the diffraction problem. For $\theta = 0.7°$ and for TE polarization, these two peaks disappear and the loss spectrum is nearly identical to that achieved under normal incidence. This is again understood from the SP picture of Fig. 11(a). For TE polarization, SP pattern (2) cannot be excited because its polarization is orthogonal to that of the incident plane wave.

Figure 11(c) shows the absorption losses of the silver membrane for $\theta = 0.7°$, $\delta = 0°$, and TM polarization and for different grating depths. One sees that the losses associated

to the hole resonance (for $\lambda \approx 0.8 \ \mu$m) strongly depend on the grating depth, whereas the losses associated to the resonant excitation of counterpropagative SPs with opposite amplitudes is only weakly dependent on the depth. This clearly evidences that the excitation of the SP pattern formed by two counterpropagative SP is mainly a property of the isolated interface and not of the full membrane.

V. CONCLUSION

In conclusion, a perturbative approach for SP-related phenomena of isolated metallodielectric interfaces corrugated by subwavelength defects has been presented. It provides simple physical pictures which help understanding different and complex SP-related effects. For instance, for one-dimensional or two-dimensional metallic membranes perforated by subwavelength aperture, the perturbative approach quantitatively explains the fact that the optical response of these membranes is nearly identical to that of a flat dielectric-metallic interface for frequencies corresponding to the SP momentum of flat interfaces. Consequently, the corresponding membrane transmission is very weak for these frequencies, a fact which is wrongly attributed to the Rayleigh anomaly in the literature. The theory also predicts phenomena like the SP resonance for gratings with a vertical mirror symmetry at very small (but non-null) incidences for one-dimensional or two-dimensional metallic membranes and the possible absence of any reflection when outcoupling from an array of very narrow slits to free space.

However, the perturbative approach cannot account for all SP-related phenomena on interfaces corrugated at subwavelength scales. For instance, it cannot predict the pole responsible for the remarkable transmission of two-dimensional metallic membranes perforated by subwavelength holes which corresponds to the existence of an intense field pattern inside the hole. More generally, the perturbative approach does not apply to gratings for which localized plasmons on subwavelength defects are responsible for a strong field enhancement.

From the previous analysis, one can also analyze the role of SPs in the transmission through metallic gratings with subwavelength apertures. For one-dimensional gratings, SPs are mainly responsible for two effects: the null transmission for frequencies corresponding to the SP momentum of flat interfaces and the SP resonance of gratings with a vertical mirror symmetry at very small (but non-null) incidences. Concerning the transmission, it is found that SPs have a detrimental role, in agreement with Ref. 8. It is noticeable in Fig. 2(a) that the zero-order maximum transmission MT is large ($\approx 80\%$) for any frequency below the Rayleigh cutoff, except for energies in the SP band. This is due to the excitation of the nonresonant SP pattern which results into a null coupling (coefficient τ) between the incident plane wave and the fundamental Bloch mode of the slit array. In turn, the grating transmission in the SP band varies as $T \approx (\lambda_{sp} - \lambda)^4$, resulting in a low and flat transmission over a broad spectral range. Explaining the observation of high transmission (relatively to the fraction of the slit area) by a physical mechanism relying on a capture of the incident light by SPs and on a subsequent funneling or squeezing of the SP into the slit has to our knowledge not be substantiated so far and we suspect that it may be wrong. The reverse, holds, in fact. In the SP band, the coupling between the incident wave and the Bloch mode of the slit array vanishes, resulting in a lower peak transmission. For two-dimensional membranes, the situation is radically different because of the evanescent character of the Bloch mode of the hole array. As shown in Ref. 10, the anomalous transmission results from a SP resonance of the isolated interface and especially from a large value of the pole of ρ. Note that this pole of ρ also results in a pole for the coupling coefficient τ responsible for an increase of τ by a factor 10 at the resonance. Thus, for the two-dimensional membrane, a funneling mechanism can be invoked although the prime effect is a pole of ρ which results in a zero of the denominator in a Fabry-Perot model.[10] Because this pole corresponds to a "localized" SP, it is shifted in frequency from the SP band associated to the zero of τ. In addition, note that the antisymmetric SP discussed in Sec. IV C, which results in a pole of ρ, also provides anomalous transmission. For instance, for $\theta = 2°$ and TM polarization, we calculated a peak transmission of $\approx 20\%$ for the set of parameters of Fig. 11.

The perturbative approach is general in the sense that it does not depend on the subwavelength defect geometry. This defect can be as well a deep etch in the metal as we was considered in this work, or a nonmetallic particle deposited on the interface. It could also remain valid for more random metallic structures provided that some local periodicity is conserved to excite the SP waves. We hope that these simple pictures will be useful to optimize plasmonic nanomaterials.

[1] H. Raether, *Surface Plasmons on Smooth and Rough Surfaces and on Gratings* (Springer-Verlag, Berlin, 1988).

[2] A. Hessel and A. A. Oliner, Appl. Opt. **4**, 1275 (1965); D. Maystre, in *Electromagnetic Surface Modes*, edited by A. D. Boardman (Wiley, New York, 1982), Chap. 17.

[3] M. Hutley and D. Maystre, Opt. Commun. **19**, 431 (1976).

[4] M. B. Sobnack, W. C. Tan, N. P. Wanstall, T. W. Preist, and J. R. Sambles, Phys. Rev. Lett. **80**, 5667 (1998).

[5] T. W. Ebbesen *et al.*, Nature (London) **391**, 667 (1998).

[6] S. A. Maier *et al.*, Adv. Mater. (Weinheim, Ger.) **13**, 1501 (2001).

[7] J. C. Weeber, A. Dereux, C. Girard, J. R. Krenn, and J. P. Goudonnet, Phys. Rev. B **60**, 9061 (1999).

[8] Q. Cao and Ph. Lalanne, Phys. Rev. Lett. **88**, 057403 (2002).

[9] D. E. Grupp, H. J. Lezec, T. W. Ebbesen, K. M. Pelletin, and T. Thio, Appl. Phys. Lett. **77**, 1569 (2000).

[10] L. Martin-Moreno *et al.*, Phys. Rev. Lett. **86**, 1114 (2001).

[11] J. R. Andrewartha, J. R. Fox, and I. J. Wilson, Opt. Acta **26**, 69 (1979).

[12] A. Wirgin and A. A. Maradurin, Prog. Surf. Sci. **22**, 1 (1986).

[13] P. Sheng, R. S. Stepleman, and P. N. Sanda, Phys. Rev. B **26**,

2907 (1982).

[14] S. H. Zaidi, M. Yousaf, and S. R. Brueck, J. Opt. Soc. Am. B **8**, 770 (1991).

[15] H. Lochbihler, Phys. Rev. B **50**, 4795 (1994).

[16] A. Barbara, P. Quémerais, E. Bustarret, and T. Lopez-Rios, Phys. Rev. B **66**, 161403 (2002).

[17] U. Schröter and D. Heitmann, Phys. Rev. B **58**, 15 419 (1998).

[18] M. M. J. Treacy, Appl. Phys. Lett. **75**, 606 (1999); M. M. J. Treacy, Phys. Rev. B **66**, 195105 (2002).

[19] J. A. Porto, F. J. Garcia-Vidal, and J. B. Pendry, Phys. Rev. Lett. **83**, 2845 (1999); F. J. Garcia-Vidal, and L. Martin-Moreno, Phys. Rev. B **66**, 155412 (2002).

[20] S. Astilean, Ph. Lalanne, M. Palamaru, and K. D. Möller, Opt. Commun. **175**, 265 (2000).

[21] S. Collin, F. Pardo, R. Tessier, and J. L. Pelouard, Phys. Rev. B **63**, 033107 (2001).

[22] Ph. Lalanne and G. M. Morris, J. Opt. Soc. Am. A **13**, 779 (1996).

[23] M. G. Moharam, E. B. Grann, D. A. Pommet, and T. K. Gaylord, J. Opt. Soc. Am. A **12**, 1068 (1995).

[24] J. L. Adams and L. C. Botten, J. Opt. **10**, 109 (1979).

[25] Ph. Lalanne *et al.*, J. Opt. A: Pure Appl. Opt. **2**, 48 (2000).

[26] As we checked through other computations, this phenomenon always occurs for other permittivitties or subwavelength slit widths for very small angles of incidence.

[27] N. P. Wanstall, T. W. Preist, W. C. Tan, M. B. Sobnack, and J. R. Sambles, J. Opt. Soc. Am. A **15**, 2869 (1998).

[28] F. J. Garcia-Vidal *et al.*, J. Lightwave Technol. **17**, 2191 (1999).

[29] L. Salomon, F. Grillot, A. V. Zayats, and F. de Fornel, Phys. Rev. Lett. **86**, 1110 (2001).

[30] E. Popov, M. Neviere, S. Enoch, and R. Reinisch, Phys. Rev. B **62**, 16 100 (2000); S. Enoch, E. Popov, M. Neviere, and R. Reinisch, J. Opt. A: Pure Appl. Opt. **4**, S83 (2002).

[31] K. Moller, O. Sternberg, H. Grebel and Ph. Lalanne, J. Appl. Phys. **91**, 9461 (2002).

[32] L. Li, J. Opt. Soc. Am. A **14**, 2758 (1997).